MITIGATION ATMOSPHERIC EFFECTS IN INTERFEROGRAM WITH USING INTEGRATED MERIS/MODIS DATA AND A CASE STUDY OVER SOUTHERN CALIFORNIA

WANG Xiaoqing, ZHANG Peng, SUN Zhanyi
National Geomatics Center of China, 28 Lianhuachixi Road, Haidian District, Beijing, 100830, China - (xqwang, zhangpeng, szy)@ngcc.cn

KEY WORDS: MERIS, MODIS,Integration, Interferogram correction

ABSTRACT:

Interferometric synthetic aperture radar(InSAR) , as a space geodetictechnology, had been testified a high potential means of earth observation providing a method fordigital elevation model (DEM) and surface deformation monitoring of high precision. However, the accuracy of the interferometric synthetic aperture radar is mainly limited by the effects of atmospheric water vapor. In order to effectively measure topography or surface deformations by synthetic aperture radar interferometry (InSAR), it is necessary to mitigate the effects of atmospheric water vapor on the interferometric signals. This paper analyzed the atmospheric effects on the interferogram quantitatively, and described a result of estimating Precipitable Water Vapor (PWV) from the the Medium Resolution Imaging Spectrometer (MERIS), Moderate Resolution Imaging Spectroradiometer (MODIS) and the ground-based GPS, compared the MERIS/MODIS PWV with the GPS PWV. Finally, a case study for mitigating atmospheric effects in interferogramusing with using the integration of MERIS and MODIS PWV overSouthern California is given. The result showed that such integration approach benefits removing or reducing the atmospheric phase contribution from the corresponding interferogram, the integrated Zenith Path Delay Difference Maps (ZPDDM) of MERIS and MODIS helps reduce the water vapor effects efficiently, the standard deviation (STD) of interferogram is improved by 23％ after the water vapor correction than the original interferogram.

1. INTRODUCTION

Interferometric Synthetic Aperture Radar (InSAR) is a potentially powerful technology fortopographic and ground surface deformation mapping due to its fine resolution, high measurement accuracy, all-weather and day-and-night imagingcapability.Rogers et al. reported the first application of SAR in Earth-based observations of Venus, whileGrahamwas regarded as the first to apply an InSAR system to Earth topographic mapping.

InSAR systems were then applied to Earth observation by Zebker et al.and Gabriel et al. first demonstrated the potential of differential InSAR (DInSAR) for centimeter or sub-centimeter level surface deformation mapping over large areas. With the development and gradual maturity of the technology, Recently InSAR shows its powerful advantage in detecting the remote and continuous deformation while requiring higher precision.

A major error source for repeat-pass InSAR is the phase delay in radio signalpropagation through the atmosphere, especially the part due to tropospheric water vapor. Massonnet et al.first identified such effects. Zebker et al.reported, for example, that spatial and temporalchanges of 20% in the relative humidity of the troposphere could lead up to 10 to 14 cm errors in the deformations measurement and 100 to 200m errors in retrieving topographic maps for base lines ranging 100 m. Since then, some intensive research has been carried out aiming to better understand and mitigate the effects, such as water vapor delay models based on meteorology and continuous GPS observations, permanent scatterer(PS) technology.

MODIS is a passive multi-spectrum instrument and provides a near IR water vapor product with a spatial resolution of 1 kmx1 km. Since near IR observations are sensitive to the presence of clouds, cloud-free observations are preferred. Currently, MODIS near IR water vapor values can only be collected under clear sky conditions and hence only these measurements can be applied to correct InSAR measurements. It is shown that MODIS appeared to overestimate water vapor against GPS with a scalefactor of 1.05, indicating that MODIS water vapor should be calibrated before being applied to correct InSAR water vapor effects. After calibrating using a GPS-derived linear fit model, it is found that MODIS and GPS water vapor products agreed to within 1.6 mm in terms of standard deviations. Li et al. reported that, after calibrating their scale uncertainty using GPS data, two or more MODIS near IR water vapor fields can be adopted to produce Zenith Path Delay Difference Maps (ZPDDM) for InSAR atmospheric correction, and this was designated as the GPS/MODIS integrated water vapor correction model.

The Medium Resolution Imaging Spectrometer (MERIS) is passive multi-spectrum sensor on ESA ENVISAT, an advanced polar orbiting Earth observation satellite launched on 1st March 2002. MERIS has two out of fifteen narrow spectral channels in the near IR for the remote sensing of water vapor either above land or ocean surfaces under cloud free conditions or above the highest cloud level under cloudy conditions. Spatiotemporal comparisons showed agreement between MERIS and GPS water vapor products.

Application of both the GPS/MODIS integrated and the MERIS correction to ERS/ASAR data over the Los Angeles region showed that the order of water vapor effects on interferogram can be reduced from ~10 mm to ~5 mm after correction. In this paper, with ENVISA-ASAR dataset we will compare the MERIS/MODIS PWV with the GPS PWV, and work with integration of MERIS and MODIS data to mitigate the atmospheric effects in SAR interferograms in order to improve the accuracy of displacement measurements.

2. WATER VAPOR EFFECTS

2.1 Water vapor effects on SAR interferogram

There are two expression ways ofwater vapor: (1) Integrated Water Vapor (IWV) gives the total amount of water vapor that a signal from the zenith direction would encounter. (2) Precipitable Water Vapor (PWV) is the IWV scaled by the density of water ρ

$$PWV = IWV / \rho \tag{1}$$

Signals would delay as propagation in the troposphere and ionosphere, which presented as phase shift in the radar images. For reference, the basic mathematical models for repeat-pass InSAR are as follows

$$\Delta\varphi = \frac{4\pi}{\lambda}\frac{ZWD}{\cos\theta_{\text{inc}}} \tag{2}$$

where $\Delta\varphi$ is the measured interferometric phase shift (in radians), λ is the wavelength of the radar signal (in mm, 56.6mm for ERS-1/2 and 56.3 mm for ASAR), θ_{inc} is for the radar echo signal incidence angle, and ZWD represents Zenith Wet Delay (in mm), the path delay induced by water vapor along the zenith direction. The conversion of ZWD and PWV as follow:

$$ZWD = K \cdot PWV \tag{3}$$

The factor K can be calculated by

$$K = \rho \cdot R_v \left(\frac{k_3}{T_m} + k_2 - w \cdot k_1 \right) / 10^6$$

R_v is the specific gas constant for water vapor, k_1、k_2 and k_3 are the atmospheric refractivity constants (refer to), and w=0.622 is the mass ratio of water vapor molecule to dry air molecule. T_m is the weighted mean temperature of the troposphere. The conversion factor of ZWD/PWV usually varies from 6.0 to 6.5, and is assumed to be 6.2 in Southern California.

From equation (2), phase shifts due to water vapor will increase with the incidence angle, and the average incidence angle of ASAR varies from 15o to 45.2 oat an average Envisat satellite altitude of 786km. Figure1 shows change tendencyof phase shiftdue to water vapor with increasing incident angle. For example, the phase shifts could be up to 80 radians with the incidence angle of 45 degree (250mm of ZWD), equivalent to 1.434m slant delay in the direction of radar line of sight (RLOS). For repeat-pass InSAR, considering that the phase of interferogram is the difference of phase between two different SAR images collected at time t1 and t2 respectively, the Interferometric phase delay due to water vapor for repeat-pass radars can be given based on equation (2):

$$\Delta\varphi_{ifm} = \left(\frac{4\pi}{\lambda}\frac{1}{\cos\theta_{\text{inc}}}\right)(ZWD_{t1} - ZWD_{t2}) = \left(\frac{4\pi}{\lambda}\frac{1}{\cos\theta_{\text{inc}}}\right)ZPDDM \tag{4}$$

ZWD_{t1} and ZWD_{t2} is the Zenith WetDelayat time t1 and t2respectively, $ZPDDM$ is Zenith Path Delay Difference Map produced by differencing the ZWD_{t1} and ZWD_{t2}, and assuming a standard deviation of ZWD(in mm) on each ZWDmeasurement ($\sigma ZWD_{\text{t1}} = \sigma ZWD_{\text{t2}} = \sigma ZWD$), the effect of ZWD on interferogramcan be given by:

$$\sigma\varphi_{ifm} = \left(\frac{4\pi}{\lambda}\frac{1}{\cos\theta_{\text{inc}}}\right)\sigma_{ZPDDM} \tag{5}$$

One should keep in mind that equation (5) is based on the assumption that ZWD values are uncorrelated for different SAR images when their time interval is greater than 1 day. From equation (5), an uncertainty of 1.0mm in PWV (6.2mm in ZWD)could result in an uncertainty of 0.4 fringes (i.e. 2π phase shift) in the resultant interferogram.

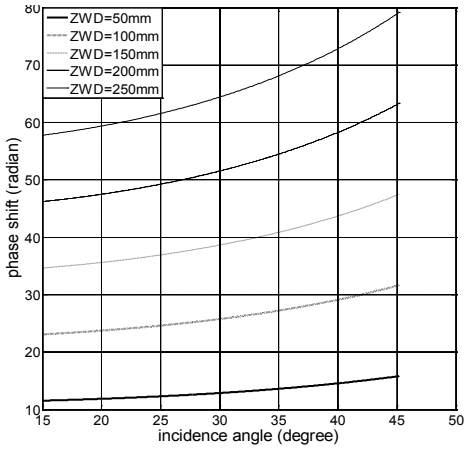

Figure1. Phase change tendencywith increasing incident angle

2.2 Water vapor effects on the DEM reconstruction and surface deformation monitoring

According to the mathematical model of topographical measurement, the relationship between elevation error and phase error for the repetitive orbital InSAR topography is as follows:

$$\sigma_h = \frac{\lambda}{4\pi}\frac{\rho\sin\theta}{B_{\perp_0}}\sigma_{\Delta\varphi} = \frac{1}{2\pi}\left(\frac{1}{2}\frac{\rho\sin\theta}{B_{\perp_0}}\right)\sigma_{\Delta\varphi} = \frac{h_a}{2\pi}\sigma_{\Delta\varphi} \tag{6}$$

Where h_a is height ambiguity, it is clear that a small height ambiguity can cause large terrain errors induced by phase errors, as well as, large baseline would result in loss of coherence between the two interference images.And the relationship between elevation error and ZWD error (e.g. residual signals after mitigating atmosphere signal with GPS/MODIS/MEIRS) is as follows:

$$\sigma_h = \frac{h_a}{2\pi}\sigma_{\Delta\varphi} = \frac{2\sqrt{2}}{\lambda}\frac{h_a}{\cos\theta_{inc}}\sigma_{\Delta ZWD} \tag{7}$$

We can evaluate the influence of the ZWD accuracy on the accuracy of obtained DEM through the above formula. For example, in order to get a DEM with a precision above 20m in case of a degree of height ambiguity of over 45m, the accuracy ZWD should be better than 8.2mm. In addition, ZWD with greater errors can still meet this requirement if the height ambiguity is smaller.

For repeated orbital deformation mapping, deformation model can be expressed asfollows:

$$\varphi_{deformation} = \frac{4\pi}{\lambda}\delta\rho_{deformation} \tag{8}$$

So the relation between deformation error and ZWD error can be given as

$$\sigma_{\delta\rho} = \frac{\sqrt{2}}{\cos\theta_{inc}}\sigma_{\Delta ZWD} \tag{9}$$

Obviously, the error of the deformation result is proportional to the ZWD error, andthe smallerincidence anglecan reduce the atmosphere influence onthe deformation monitoring result.According tothe quantitative analysis of atmospheric errors above, the influence of atmospheric effects on the topographic and deformation result can be estimatedaccurately.

3. COMPARE MODIS/MERIS PWV WITH GPS PWV

In order to verify the accuracy and availability of PWV inversed from MODIS and MERIS, the MODIS PWV and MERIS PWV are compared with PWV calculated fromground-based GPS observed data. The Southern California area is selected as the test area with the comparison of single day and temporal and spatial distribution of PWV.

3.1 MODIS PWV compared with GPS PWV

The comparison of MODIS PWV and GPS PWV of single day as follows:

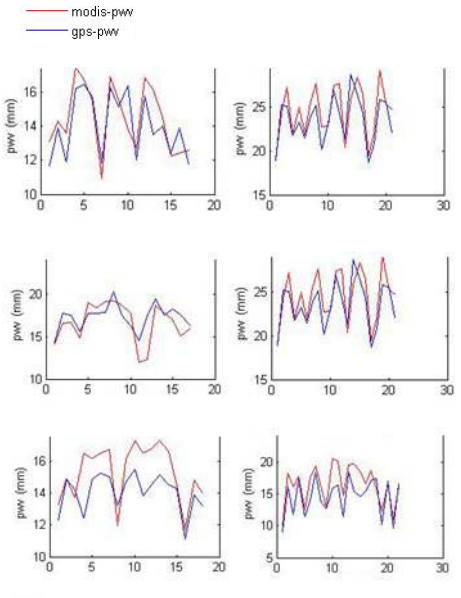

Figure2. comparison of MODIS PWV and GPS PWV of single day for 2015/6/3, 2015/6/7, 2015/6/12, 2015/6/19, 2015/6/20, 2005/10/1

And the comparison of MODIS PWV and GPS PWV of temporal and spatial distribution as follows:

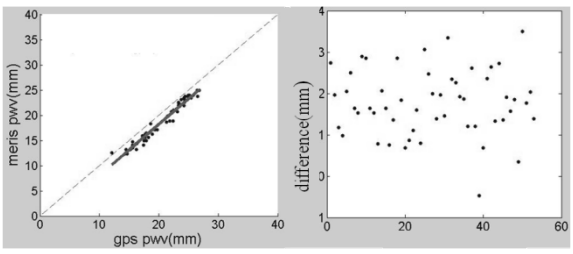

Figure3. temporal and spatial distribution comparison of MODIS PWV and GPS PWV

we can see from the figures above that there is a good linear relationship between the MODIS PWV and GPS PWV as follows: modispwv = 1.1263gps pwv - 2.1439, the Standard Deviation(STD) is 1.16mm, and the difference between the MODIS PWV and GPS PWV is mostly within the 3mm.

3.2 MERIS PWV compared with GPS PWV

The comparison of MERIS PWV and GPS PWV of single day as follows:

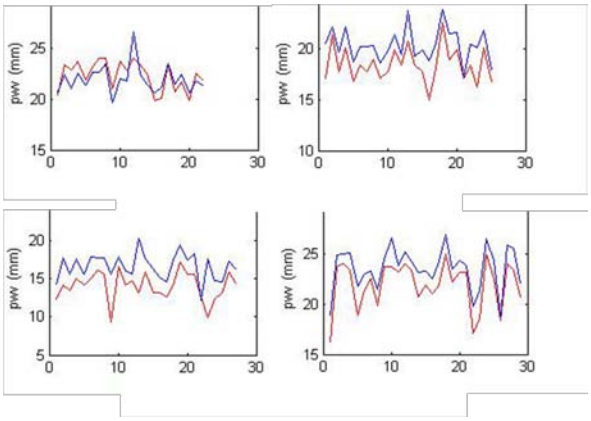

Figure4. comparison of MERIS PWV and GPS PWV of single day for 2015/6/8, 2015/6/14, 2015/6/18, 2015/10/1

And the comparison of MODIS PWV and GPS PWV of temporal and spatial distribution as follows:

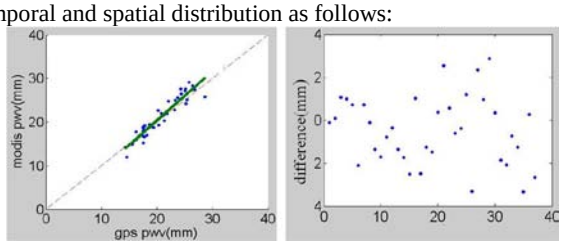

Figure5. temporal and spatial distribution comparison of MERIS PWV and GPS PWV

we can see from the figures above that there is also a good linear relationship between the M ERIS PWV and GPS PWV as follows: merispwv=0.9907gps pwv-1.5948, the Standard Deviation(STD) is 0.9277mm, and the difference between the MERIS PWV and GPS PWV is mostly within the 3mm.

The comparison shows that the accuracy of the MERIS/MODIS PWV is testified by the GPSPWV inversed by the groundobservation , and the MERIS/MODIS PWV can be used to reduce the influence of interferogram.

4. CASE STUDY: MITIGATINGATMOSPHERIC EFFECTS ON THE INTERFEROGRAM

4.1 IntegrationAtmospheric Effects of MODIS and MERIS water vapor

It is clear that MODIS and MERIS near IR water vapor products arecomplementary for correcting interferogram and it is expected that the combination ofMODIS and MERIS near IR water vapor products can expand the application ofMERIS and MODIS data for InSAR atmospheric correction. Based on our research experienceonGPS/MODIS and GPS/ MERIS integrated watervapor correction model, when both MERIS and MODIS data are available for one orboth dates and the impact of time difference between them can be considerednegligible, simple averaging of both water vapor fields is expected to reduce the noise. If the noise level in two water vapor fields is the same, averaging of these independentimages can statistically reduce the noise of the original individual water vapor fieldsby a factor of $\sqrt{2}$.

In this paper, the water vapor correction model integrated MERIS and MODIS data for InSAR atmospheric correctioncan be described as follow：

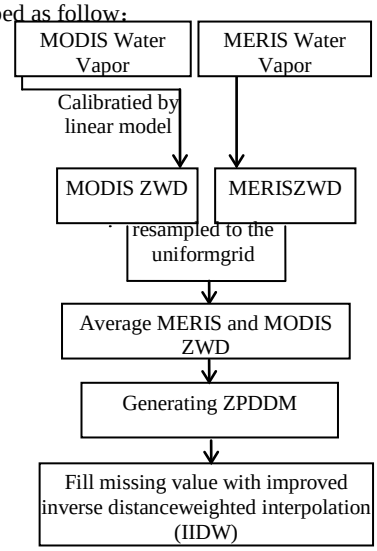

Figure6. Flowchart of ZPDDM processing with integrated MERIS and MODIS

In order to suppress the inherent noise of MERIS and MODIS measurements, alow-pass filter can be applied to the ZPDDM such as a boxcar averaging window with awidth of 2.0 km. This averaging window width is selected based on the revolution of the two data.

4.2 Application of integrated water vapor overSouthern California

Two descending ASAR images were acquired on 18th Jun 2005 and 1stOct 2005 over Southern California. The perpendicular baseline of these two ASAR images was 230m. The ASAR images were processed with the GAMMA software. Topographic effect was removed from the interferogram using a SRTM DEM with a spatial resolution of 90m. Therefore, we expect the topographic residual phased due to the DEM errors to be negligible.

Figure3 shows original interferogram and figure4 is the ZPDDM derived from average of MODIS and MERIS (process is shown as figure1) corresponding to interferogram. Figure5 shows the corrected interferogram after corrected by MERIS and MODIS integrated water vapor.

It should be noted that areas A and B, where water vapor changes are so significantly, are obviously corrected. Figure6 compares the original/corrected interferogram and ZPDDM at cross-section (a-b), which is effected seriously by water vapor. As one can see, even there are about 3.5cm water vapor delay at some pixels are mitigated. After correction, most interferogram phases are reduced that are close to zero. The standard deviation (STD) of interferogram is decreased from 1.35cm to 1.04cm after the water vapor correction, and the improvement of using MERI/MODIS is up to 23%.

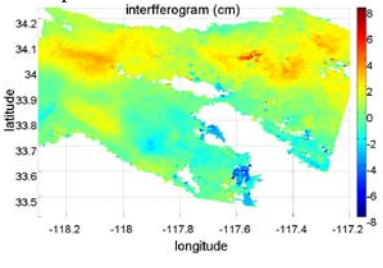

Figure7. Original interferogram

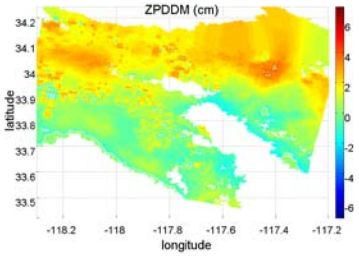

A

Figure8. Zenith Path Delay Difference Map derived from MODIS and MERIS

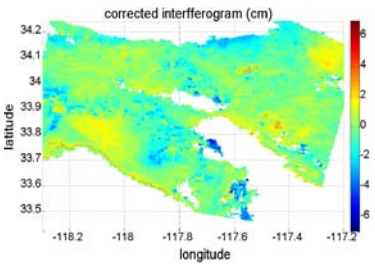

Figure9. Corrected interferogram

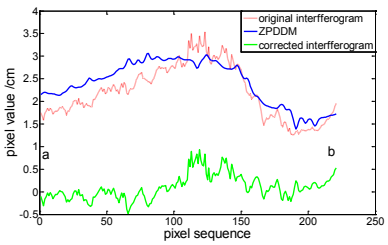

Figure10. Comparison of original/corrected interferogram and ZPDDM at cross-section（a-b）

5. CONCLUSIONS

InSAR techniques can provide deformation measurements at fine resolution (e.g. tens of metres) over wide areas (e.g. 100 km × 100 km). However, the accuracy of InSAR derived deformation signals is limited to centimetre level due to the spatiotemporal variations of atmospheric water vapor. This paper demonstratesa successful application of integrated correction with MODIS and MERIS water vapor productsof ENVISAT ASAR interferograms over southern California. The quality of interferogram phases was improved by 23%.

Thisintegration approach is capable ofremoving or reducing the atmospheric phase contribution from the corresponding interferogram. And the experiment performed with ENVISAT data over Southern California shows itis feasible to helpreduce water vapor effects efficiently. The presented method canreduce the noise of the original individual water vapor fieldsby a factor of $\sqrt{2}$, in case ofthe noise level oftwo water vapor fields from MODIS/MERIS is the same.

REFERENCES

Tang W, Liao M, Zhang L, et al. High-spatial-resolution mapping of precipitable water vapour using SAR interferograms, GPS observations and ERA-Interim reanalysis[J]. Atmospheric Measurement Techniques, 2016, 9:1-24.

Tang W, Liao M, Zhang L, et al. Atmospheric water vapor mapping by combining interferometric synthetic aperture radar and GPS observations[C]// Geoscience and Remote Sensing Symposium. IEEE, 2016:6887-6889.

Zhi-Xin H E, Jiang Y, Zhang S, et al. Application of assimilated GPS/PWV data to the rainstorms forecast over Anhui province[J]. Journal of Meteorology & Environment, 2017.

Mao M, Wang L, Zhang S, et al. Correlation Analysis Among GPS-SNR, Precipitation and GPS-PWV[J]. 2017.

Mateus P, Nico G, Catalao J. Assimilation of Sentinel-1 estimates of Precipitable Water Vapor (PWV) into a Numerical Weather Model for a more accurate forecast of extreme weather events[C]// EGU General Assembly Conference. EGU General Assembly Conference Abstracts, 2017.

Cheng S, Perissin D, Lin H, et al. Atmospheric delay analysis from GPS meteorology and InSAR APS[J]. Journal of Atmospheric and Solar-Terrestrial Physics, 2012, 86(5):71-82.

Gong W, Meyer F J, Webley P. Water Vapor Products from Differential-InSAR with Auxiliary Calibration Data: Accuracy and Statistics[C]// AGU Fall Meeting. AGU Fall Meeting Abstracts, 2014.

Webley P W, Bingley R M, Dodson A H, et al. Atmospheric Water Vapor Correction to InSAR Surface Motion Measurements in Mountains: Results from a Dense GPS Network in Mount Etna. J. Physics and Chemistry of the Earth, 2012, 27: 363-370

Hooper A, Zebker H, Segall P, et al. A new method for measuring deformation on volcanoes and other natural terrains using InSAR persistent scatters. J. Geophys. Res., 2004, 31: 236-240

Li Z H, Muller J P, Cross P, et al. Assessment of the potential of MERIS near-infrared water vapor products to correct ASAR interferometric measurements. International Journal of Remote Sensing, 2006, 27 (1-2): 349-365

Li, Z., J.-P. Muller, P. Cross, P. Albert, J. Fischer, and R. Bennartz (2006). Assessment of the potential of MERIS near-infrared water vapor products to correct ASAR interferometric measurements, Int. J. Remote Sens., 27, 349-365.

Li, ZW. Modeling atmospheric effects on repeat-pass InSAR measurements. Ph.D Dissertation, The Hong Kong Polytechnic University, Hong Kong, 2005.

ACKNOWLEDGMENTS:
This work was supported by the National Natural Science Foundation of China (grant number 41504020), Natural Science Foundation of Tianjin City (grant number 16JCZDJC40400)